PSR J1909−3744, a Binary Millisecond Pulsar with a Very Small Duty Cycle

B. A. Jacoby[1], M. Bailes[2], M. H. van Kerkwijk[3], S. Ord[2], A. Hotan[2,4], S. R. Kulkarni[1], and S. B. Anderson[1]

ABSTRACT

We report the discovery of PSR J1909−3744, a 2.95 millisecond pulsar in a nearly circular 1.53 day orbit. Its narrow pulse width of 43 μs allows pulse arrival times to be determined with great accuracy. We have spectroscopically identified the companion as a moderately hot ($T \approx 8500$ K) white dwarf with strong absorption lines. Radial velocity measurements of the companion will yield the mass ratio of the system. Our timing data suggest the presence of Shapiro delay; we expect that further timing observations, combined with the mass ratio, will allow the first accurate determination of a millisecond pulsar mass. We have measured the timing parallax and proper motion for this pulsar which indicate a transverse velocity of 140^{+80}_{-40} km s^{-1}. This pulsar's stunningly narrow pulse profile makes it an excellent candidate for precision timing experiments that attempt to detect low frequency gravitational waves from coalescing supermassive black hole binaries.

Subject headings: binaries:close — pulsars: individual(PSR J1909−3744) — relativity — stars: distances — stars: neutron — white dwarfs

1. INTRODUCTION

Binary radio pulsars provide a rich laboratory for a wide range of physical inquiry, including neutron star masses and the evolution of binary systems. The pulsars with the best-determined masses all have eccentric relativistic orbits, spin periods of tens of milliseconds,

[1]Department of Astronomy, California Institute of Technology, MS 105-24, Pasadena, CA 91125; baj@astro.caltech.edu, srk@astro.caltech.edu, sba@astro.caltech.edu.

[2]Centre for Astrophysics and Supercomputing, Swinburne University of Technology, P.O. Box 218, Hawthorn, VIC 31122, Australia; mbailes@swin.edu.au, sord@swin.edu.au, ahotan@swin.edu.au.

[3]Department of Astronomy and Astrophysics, University of Toronto, 60 St. George Street, Toronto, ON M5S 3H8, Canada; mhvk@astro.utoronto.ca.

[4]Australia Telescope National Facility, CSIRO, P.O. Box 76, Epping, NSW 1710, Australia.

and masses clustered very tightly around $1.35\,M_\odot$ (Thorsett & Chakrabarty 1999; Bailes et al. 2003). It is generally thought that millisecond pulsars ($P \leq 10\,\mathrm{ms}$) should have greater mass than these longer-period pulsars due to a larger accreted mass. There is indeed a statistical suggestion that this is the case, but to date no precise millisecond pulsar mass measurements exist. Currently, the best-determined millisecond pulsar masses are $m_\mathrm{p} = 1.57^{+0.12}_{-0.11}\,M_\odot$ for PSR B1855+09 (Nice et al. 2003) and $m_\mathrm{p} = 1.58 \pm 0.18\,M_\odot$ for PSR J0437−4715 (van Straten et al. 2001).

PSR J1909−3744 was discovered during the Swinburne High Latitude Pulsar Survey, a recently-completed pulsar search using the 13-beam multibeam receiver on the 64-m Parkes radio telescope (Jacoby 2003; Jacoby et al. in preparation). This survey is similar to, and an extension of, the highly-successful Swinburne Intermediate Latitude Pulsar Survey (Edwards et al. 2001; Edwards & Bailes 2001a,b). The pulsar was discovered in three adjacent survey beams observed on 2001 January 25 and confirmed on 2001 May 26. Due to the pulsar's strong broad-band scintillation, the initial position inferred from the discovery data was in error by nearly a full beamwidth; it was not until we obtained a phase-connected timing solution that we realized the correct position.

Among the properties that can make a pulsar useful for precision timing experiments are a bright, narrow pulse profile, extremely stable rotation, proximity to the earth, and a companion star which can be detected and studied. PSR J1909−3744 appears to possess all of these desirable traits. Nearly all of the pulsar's flux comes in a single narrow, sharp peak with full-width half-maximum (FWHM) of only $43\,\mu$s, less than 1.5% of the 2.95 ms pulse period (Fig. 1). The brightness of the pulsar varies by at least a factor of 30 in the 21-cm band. The mean flux density of our observations is 3 mJy, but this is biased by the fact that we tend to observe longer when the pulsar is bright. Extremely high precision timing observations are possible during episodes of favorable scintillation.

2. PULSE TIMING

Following the confirmation of PSR J1909−3744, we began timing observations with the $2 \times 512 \times 0.5\,\mathrm{MHz}$ Parkes filterbank centered on 1390 MHz. As a result of our incorrect discovery position, few observations taken before February 2002 yielded data useful for high-precision timing. Integration times ranged from three to 100 minutes, with the longer observations broken into 10-minute sub-integrations.

We followed standard pulsar timing procedures: folded pulse profiles from individual observations were cross-correlated with a high signal-to-noise template profile to determine

an average pulse time of arrival (TOA), corrected to UTC(NIST). The standard pulsar timing package TEMPO[5], along with the Jet Propulsion Laboratory's DE405 ephemeris, was used for all timing analysis. All 1.4 GHz TOAs with uncertainty less than 1 μs were included. TOA uncertainties were multiplied by 1.25 to achieve reduced $\chi^2 \simeq 1$. Several observations were also obtained in the 50-cm band with the $2 \times 256 \times 0.125$ MHz Parkes filterbank centered on 660 MHz. As these observations did not yield TOA uncertainties less than 1 μs they were used only to determine the dispersion measure (DM), which was then held fixed.

Because of the system's low eccentricity (e), we used the ELL1 binary model which replaces the familiar longitude of periastron (ω), time of periastron (T_0), and e with the time of ascending node ($T_{\rm asc}$) and the Laplace-Lagrange parameters $e \sin\omega$ and $e \cos\omega$ (Lange et al. 2001). We give the results of our timing analysis in Table 1 and show residuals relative to this best-fit model in Figure 2. The weighted RMS residual is only 330 ns, among the best obtained for any pulsar over $\sim$2 year timespans.

We have begun regular observations of PSR J1909−3744 with the Caltech-Parkes-Swinburne Recorder II (CPSR2; Bailes 2003). CPSR2 is a baseband recorder and real-time coherent dedispersion system with two dual-polarization bands, each 64 MHz wide. The CPSR2 pulse profile shown in Figure 1 is smeared by only 2 μs, compared with the 82 μs time resolution of the 512-channel filterbank. Initial results from CPSR2 data show great promise for high precision timing, and will be reported in a future paper.

2.1. Shapiro Delay

Though our current data set suffers from poor orbital phase coverage (specifically a lack of high-quality observations near inferior conjunction), we find strong evidence of Shapiro delay. If we remove Shapiro delay (i.e. companion mass, $m_{\rm c}$, and sine of orbital inclination, $\sin i$) from the timing model and allow TEMPO to optimize the remaining parameters, χ^2 increases from 98.8 to 128.1 (for 102 and 104 degrees of freedom respectively), indicating a highly significant detection. The peak-to-peak residual is essentially the same in either case (3.4 μs) as much of the Shapiro delay signal is absorbed into an erroneously large Roemer delay; however, the weighted RMS residual increases to 370 ns when the model excludes $m_{\rm c}$ and $\sin i$. Holding the astrometric, orbital, and spin parameters fixed at the values in Table 1 but neglecting Shapiro delay increases the peak-to-peak residual to 8.1 μs, with pulses observed nearest inferior conjunction arriving later than predicted by the model.

[5]http://pulsar.princeton.edu/tempo

Given its large uncertainty, we are not concerned by the most likely value of $\sin i > 1$ found by TEMPO's linear least-squares fit. To confirm that the Shapiro delay is physically meaningful, we constructed a χ^2 map as a function of m_c and $\sin i$, while optimizing the remaining parameters. Our sparse data set is consistent with a large range of allowed parameter space, constraining the system to have $\sin i \geq 0.85$ and $0.17\,M_\odot \leq m_c \leq 0.55\,M_\odot$ (95% confidence). The covariance of the poorly-determined m_c and $\sin i$ with the projected semimajor axis ($a \sin i$) and e means that the uncertainties in these parameters given in Table 1 are likely to be underestimated.

Currently, the strongest constraint on the companion mass is the minimum mass of $0.195\,M_\odot$ obtained from the mass function by assuming $i = 90°$ and $m_p = 1.4\,M_\odot$; the fact that Shapiro delay is detected at all suggests that we are likely viewing the system roughly edge-on. Future pulsar timing observations near inferior conjunction will significantly improve the Shapiro delay-derived companion mass.

2.2. Distance

We have measured the parallax, $\pi = 1.22 \pm 0.44$ mas, and hence can estimate the distance to PSR J1909−3744, $d_\pi = 0.82^{+0.46}_{-0.22}$ kpc. Combined with the proper motion, this distance corresponds to a transverse velocity of $140^{+80}_{-40}\,\mathrm{km\,s^{-1}}$. The DM-derived distance estimate is 0.46 kpc (Cordes & Lazio 2002).

The pulsar's proper motion induces an apparent radial acceleration equal to $\mu^2 d/c$ (Shklovskii 1970). This secular acceleration will allow an entirely independent distance estimate from precise measurement of the orbital period derivative, $\dot{P}_b$ (Bell & Bailes 1996). For circular binaries such as PSR J1909−3744, the intrinsic $\dot{P}_b$ due to general relativity is negligible. However, the secular acceleration will eventually produce a measurable $\dot{P}_b$ which can be used to determine the distance. The peak-to-peak timing signal due to parallax is $\sim 1.4\,\mu$s, while the $\dot{P}_b$ signal increases with the observing baseline, t, as $\sim 240\,\mathrm{ns}\,(t/1\,\mathrm{yr})^2$. Thus, after only a few years of timing $\dot{P}_b$ will give the more precise distance. We note that the acceleration induced by differential Galactic rotation is about two orders of magnitude smaller than the secular acceleration.

The secular acceleration also corrupts the observed period derivative ($\dot{P}$). Since the pulsar's intrinsic spindown rate ($\dot{P}_{int}$) is non-negative, we can obtain an upper distance limit of 1.4 kpc, consistent with the measured parallax. Conversely, the measured proper motion and parallax-derived distance allow us to correct $\dot{P}$ for the secular acceleration and hence determine $\dot{P}_{int}$.

3. OPTICAL OBSERVATIONS OF THE WHITE DWARF COMPANION

At the position of the pulsar, the digitized sky survey plates showed a possible counterpart. To verify this, we obtained images on the night of 2003 June 4 with the Magellan Instant Camera (MagIC) at the 6.5-m Clay telescope on Las Campanas. We took a 10-min exposure in B and a 5-min exposure in R. The conditions were poor, with thin clouds and $1''$ seeing.

The images were reduced using the Munich image data analysis system (MIDAS), following the usual steps of bias subtraction (separately for the four amplifiers) and flat-fielding using dome flats. For the astrometric calibration, we selected 58 USNO-B1.0 (Monet et al. 2003) objects that overlapped with our images, were not overexposed, and appeared stellar. For these objects, we measured centroids and fitted for zero-point position, plate scale, and position angle. Rejecting 23 outliers with residuals larger than $0\farcs5$, the inferred single-star measurement error in both bands is $0\farcs15$ in each coordinate, which is consistent with expectations for the USNO-B1.0 measurements. Hence our astrometry should be tied to the USNO-B1.0 system at the $\sim 0\farcs03$ level.

In both images, we found an object near the position of the pulsar which is blue relative to other stars in the field; see Fig. 3. The position inferred from our astrometry is $\alpha_{\rm J2000} = 19^{\rm h}09^{\rm m}47\fs457$, $\delta_{\rm J2000} = -37^\circ 44' 14\farcs17$, which is consistent with the timing position listed in Table 1 within the uncertainty with which the USNO-B1.0 system is tied to the International Celestial Reference Frame ($\sim 0\farcs2$ in each coordinate).

The identification of this object with the pulsar's companion was confirmed by spectra, taken on the night of 2003 June 6, using the Low Dispersion Survey Spectrograph 2 (LDSS2) at the Clay telescope. We took two 30-min exposures with the high resolution grism and a $1''$ slit, which gives a resolution of ~ 6 Å. The conditions were mediocre, with thin cirrus and $0\farcs7$ seeing.

We used MIDAS to reduce the spectra. They were bias-subtracted and flat-fielded using normalized dome flats (in which the noisy blue part was set to unity). After sky subtraction, the two spectra were extracted using optimal weighting, and added together. To derive the response, we used spectra of Feige 110, taken during the same night, and fluxes from calibrated STIS spectra.[6] The result is shown in Fig. 4. We stress that since cirrus was present, the absolute flux calibration is not reliable, although both from the spectrum and from a rough photometric calibration using USNO-B1.0 magnitudes, it follows that the companion has $V \simeq 21$.

[6]See http://www.stsci.edu/instruments/observatory/cdbs/calspec.html.

The spectrum (Fig. 4) shows only the Balmer lines of Hydrogen, from Hα up to H10, consistent with a DA white dwarf of low surface gravity (and thus low mass). The strength of the lines and the slope of the spectrum are similar to what is seen for PSR J1012+5307 (van Kerkwijk et al. 1996) and PSR J0218+4232 (Bassa et al. 2003), indicating a similar temperature of $\sim$8500 K.[7]

Assuming a mass of $\sim 0.20\,\mathrm{M}_\odot$, the white dwarf should have a radius of approximately $0.03\,\mathrm{R}_\odot$ and a luminosity of $\sim 4 \times 10^{-3}\,\mathrm{L}_\odot$ (Driebe et al. 1998; Rohrmann et al. 2002). The corresponding absolute magnitude is $M_V \simeq 11.0$, which implies $V \simeq 20.5$ at a distance of 0.8 kpc, consistent with the rough photometry quoted above.

4. CONCLUSIONS

Pulse timing precision is often limited by systematic errors that distort the shape of pulsar profiles due to the interstellar medium and imperfect polarimetric and instrumental response. Intrinsically narrow pulses are less susceptible to these errors, as are pulsars with small dispersion measures. PSR J1909−3744 is likely to become a cornerstone of future timing array experiments to detect low-frequency gravitational waves. It is noteworthy that PSR J1909−3744 is far from other high-precision pulsars on the sky and therefore probes a unique line of sight.

In the shorter run, further timing of the pulsar, especially with CPSR2, should yield an accurate inclination and a reasonably precise companion mass. Furthermore, in a modest spectroscopic observing campaign on an 8-m class telescope, the radial velocity orbit of the companion can be measured precisely. These combined results should allow a very reliable pulsar mass measurement, and advance our understanding of binary pulsar evolution and recycling.

We thank R. Edwards for invaluable help with pulsar search software, H. Knight for assistance with Parkes observations, and M. Hamuy, V. Mariño, and M. Roth for help with the Magellan observations. BAJ and SRK thank NSF and NASA for supporting their research. MHvK acknowledges support by the National Sciences and Engineering Research Council of Canada. The Parkes telescope is part of the Australia Telescope which is funded by the Commonwealth of Australia for operation as a National Facility managed by CSIRO.

[7]This high temperature may be surprising, given the pulsar's long characteristic age of roughly 8 Gyr. It indeed sets interesting constraints on the thickness of the outer Hydrogen envelope of the white dwarf; for a discussion and references, see Bassa et al. (2003).

REFERENCES

Bailes, M. 2003, in ASP Conf. Ser. 302, Radio Pulsars, ed. M. Bailes, D. J. Nice, & S. E. Thorsett (San Francisco: ASP), 57

Bailes, M., Ord, S. M., Knight, H. S., & Hotan, A. W. 2003, ApJ, 595, L49

Bassa, C. G., van Kerkwijk, M. H., & Kulkarni, S. R. 2003, A&A, 403, 1067

Bell, J. F. & Bailes, M. 1996, ApJ, 456, L33

Cordes, J. M., & Lazio, T. J. W. 2002, preprint (astro-ph/0207156)

Driebe, T., Schoenberner, D., Bloecker, T., & Herwig, F. 1998, A&A, 339, 123

Edwards, R. T. & Bailes, M. 2001a, ApJ, 547, L37

—. 2001b, ApJ, 553, 801

Edwards, R. T., Bailes, M., van Straten, W., & Britton, M. C. 2001, MNRAS, 326, 358

Jacoby, B. A. 2003, in ASP Conf. Ser. 302, Radio Pulsars, ed. M. Bailes, D. J. Nice, & S. E. Thorsett (San Francisco: ASP), 133

Lange, C., Camilo, F., Wex, N., Kramer, M., Backer, D., Lyne, A., & Doroshenko, O. 2001, MNRAS, 326, 274

Monet, D. G., et al. 2003, AJ, 125, 984

Nice, D., Splaver, E. M., & Stairs, I. H. 2003, in ASP Conf. Ser. 302, Radio Pulsars, ed. M. Bailes, D. J. Nice, & S. E. Thorsett (San Francisco: ASP), 75

Rohrmann, R. D., Serenelli, A. M., Althaus, L. G., & Benvenuto, O. G. 2002, MNRAS, 335, 499

Shklovskii, I. S. 1970, Sov. Astron., 13, 562

Thorsett, S. E. & Chakrabarty, D. 1999, ApJ, 512, 288

van Kerkwijk, M. H., Bergeron, P., & Kulkarni, S. R. 1996, ApJ, 467, L89

van Straten, W., Bailes, M., Britton, M., Kulkarni, S. R., Anderson, S. B., Manchester, R. N., & Sarkissian, J. 2001, Nature, 412, 158

Table 1. Parameters of the PSR J1909−3744 system.

Parameter	Value[a]
Right ascension, $\alpha_{\rm J2000}$	$19^{\rm h}09^{\rm m}47\overset{\rm s}{.}44008(2)$
Declination, $\delta_{\rm J2000}$	$-37^\circ44'14\overset{''}{.}226(1)$
Proper motion in α, μ_α (mas yr^{-1})	−9.6(2)
Proper motion in δ, μ_δ (mas yr^{-1})	−35.6(7)
Annual parallax, π (mas)	1.22(44)
Pulse period, P (ms)	2.9471080205034(1)
Period derivative, $\dot{P}$ (10^{-20})	1.4026(3)
Reference epoch (MJD)	52055.8704
Dispersion measure, DM (pc cm^{-3})	10.394(1)
Binary period, $P_{\rm b}$ (d)	1.5334494503(1)
Projected semimajor axis, $a\sin i$ (lt-s)	1.897992(4)
$e\sin\omega$ ($\times10^{-7}$)	0.1(90)
$e\cos\omega$ ($\times10^{-7}$)	−2.6(17)
Time of ascending node, $T_{\rm asc}$ (MJD)	52055.87046667(6)
$\sin i$	1.1(4)
Companion mass $m_{\rm c}$ ($M_\odot$)	0.13(37)
Derived Parameters	
Mass function, $f(m)$	0.00312196(2)
Orbital eccentricity, e ($\times10^{-7}$)	2.6(18)
Longitude of periastron, ω (deg)	177.874428 ± 190
Time of periastron, T_0	52056.6281373 ± 0.8
Parallax distance, d_π (kpc)	$0.82^{+0.46}_{-0.22}$
Transverse velocity, $v_\perp$ (km s^{-1})	140^{+80}_{-40}
Intrinsic period derivative, $\dot{P}_{\rm int}$ (10^{-20})[b]	$0.61^{+0.23}_{-0.50}$
Surface magnetic field, $B_{\rm surf}$ ($\times10^8$G)[b]	$1.3^{+0.2}_{-0.8}$
Characteristic age, $\tau_{\rm c}$ (Gyr)[b]	$7.7^{+35.0}_{-2.1}$
Galactic longitude, l (deg)	359.73
Galactic latitude, b (deg)	−19.60
Distance from Galactic plane, $\lvert z\rvert$ (kpc)	$0.28^{+0.16}_{-0.07}$
Pulse FWHM, w_{50} (μs)	43
Pulse width at 10% peak, w_{10} (μs)	89

[a]Figures in parenthesis are uncertainties in the last digit quoted. Uncertainties are calculated from twice the formal error produced by TEMPO.

[b]Corrected for secular acceleration based on measured proper motion and parallax.

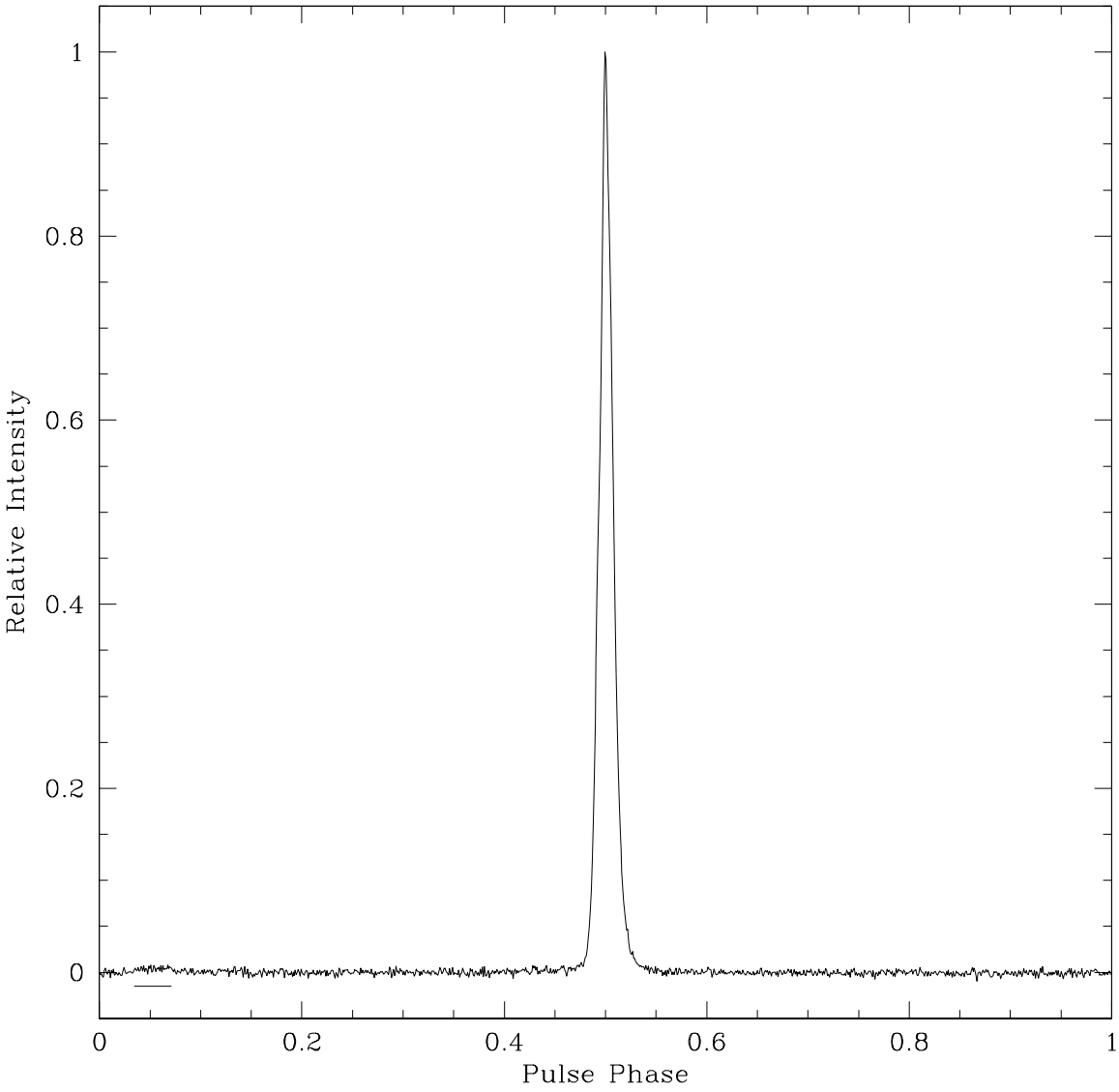

Fig. 1.— Coherently-dedispersed average pulse profile of PSR J1909−3744 at 1341 MHz as measured by the CPSR2 baseband system. Instrumental smearing is just 2μs. The location of a very weak interpulse is indicated by the underscore at left.

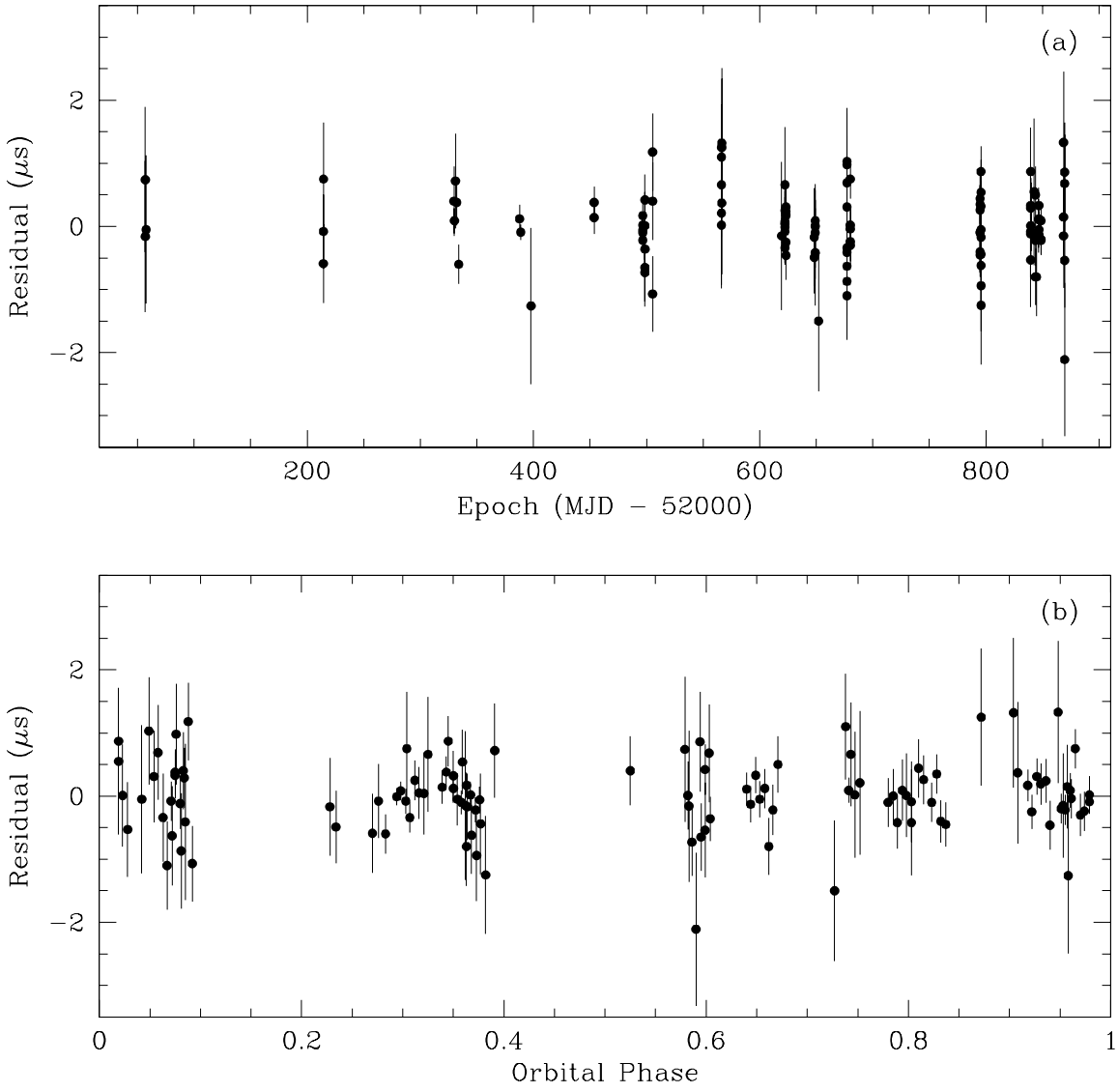

Fig. 2.— Timing residuals for PSR J1909−3744. (a): Residuals vs. observation epoch. (b): Residuals vs. orbital phase. Inferior conjunction occurs at orbital phase 0.16.

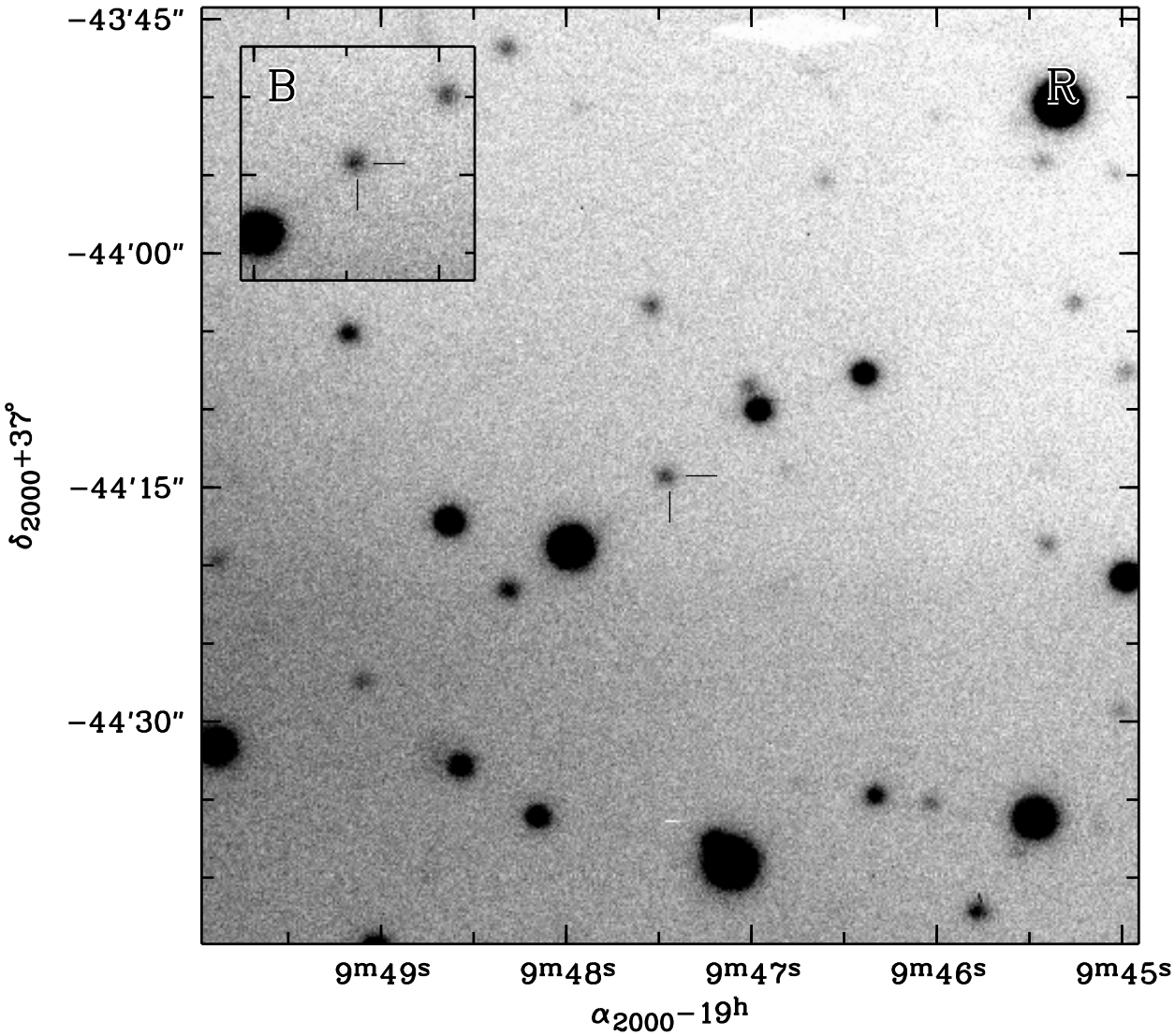

Fig. 3.— Image of the field of PSR J1909−3744. The large frame shows our R-band image; the position of the pulsar is indicated by the tick marks. The inset shows the B-band image; compared to other stars in the field, the companion is blue.

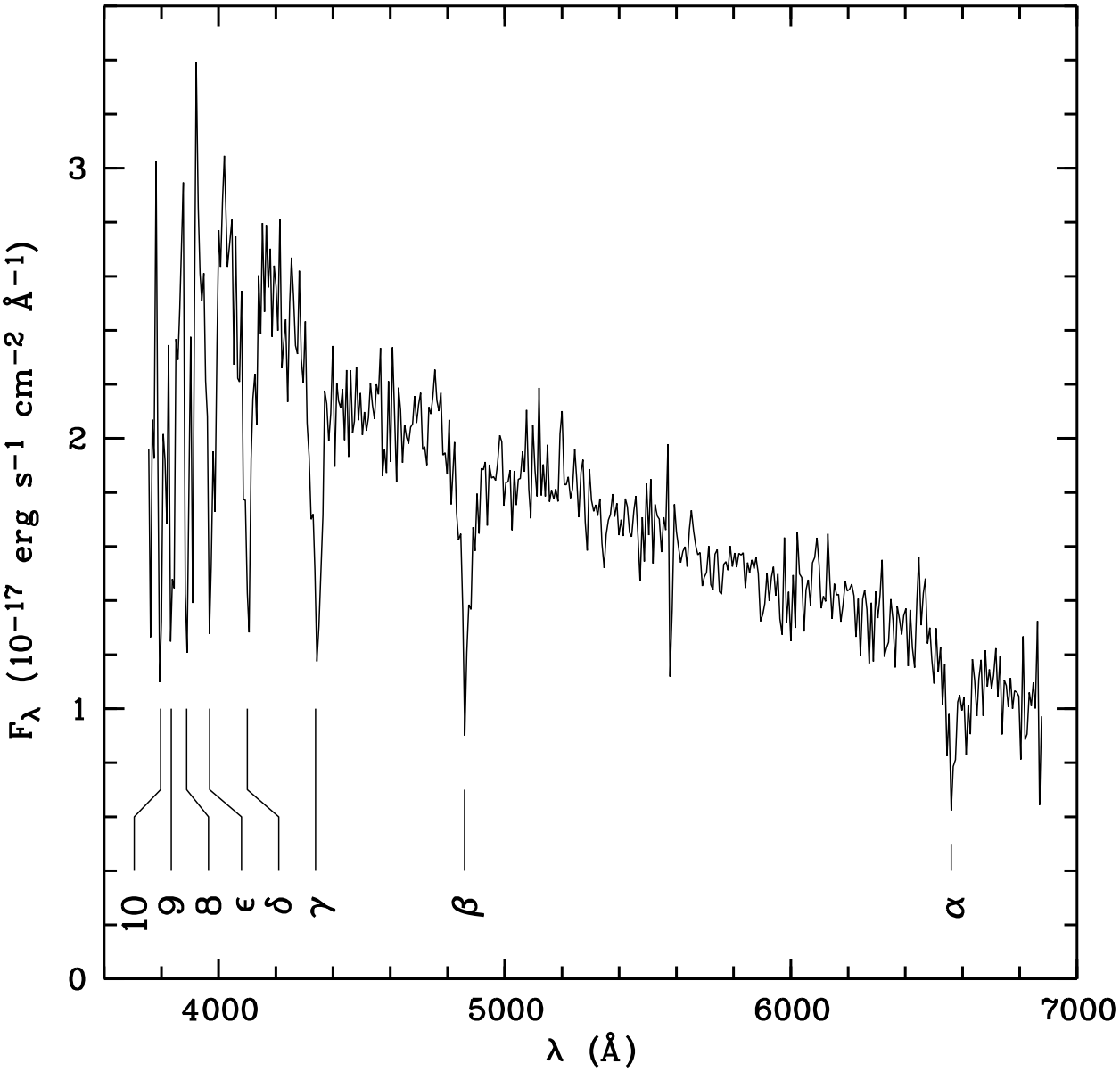

Fig. 4.— Spectrum of the companion of PSR J1909−3744, showing that it is a low-mass DA white dwarf. The Balmer lines from Hα to H10 are indicated. Note that the absolute flux calibration is uncertain by about 50%, as cirrus was present during the observations. The relative calibration, however, should be reliable (except longward of ~ 6400 Å, where the spectrum might be contaminated by second-order light).